# Transcriptome sequencing reveals PCAT5 as a novel ERG-regulated long non-coding RNA in prostate cancer

Antti Ylipää[1,2], Kati Kivinummi[1,2,3], Annika Kohvakka[2,3], Matti Annala[1,2], Leena Latonen[2,3], Mauro Scaravilli[2,3], Kimmo Kartasalo[1,2], Simo-Pekka Leppänen[1,2], Serdar Karakurt[2,3], Janne Seppälä[1,2], Olli Yli-Harja[1,3], Teuvo L.J. Tammela[4], Wei Zhang[5], Tapio Visakorpi[2,3], Matti Nykter[1,2]

[1]Department of Signal Processing, Tampere University of Technology, Tampere, Finland; [2]Institute of Biosciences and Medical Technology - BioMediTech, University of Tampere, Tampere, Finland; [3]Fimlab Laboratories, Tampere University Hospital, Tampere, Finland; [4]Department of Urology, Tampere University Hospital and Medical School, University of Tampere, Tampere, Finland; [5]Department of Pathology, University of Texas M.D. Anderson Cancer Center, Houston, TX, USA

## Conflicts of interest

The authors declare no conflicts of interest.

## Abstract

Castration-resistant prostate cancer (CRPC) that arise after the failure of androgen blocking therapies cause most of the deaths from prostate cancer (PC), intensifying the need to fully understand CRPC pathophysiology. In this study, we characterized the transcriptomic differences between untreated PC and locally recurrent CRPC. Here we report the identification of 145 previously unannotated intergenic long non-coding RNA transcripts (lncRNA) or isoforms that are associated with PC or CRPC. Of the one-third of these transcripts that were specific for CRPC, we defined a novel lncRNA termed PCAT5 as a regulatory target for the transcription factor ERG, which is activated in ~50% of human PC. Genome-wide expression analysis of a PCAT5-positive PC after PCAT5 silencing highlighted alterations in cell proliferation pathways. Strikingly, an in vitro validation of these alterations revealed a complex integrated phenotype affecting cell growth, migration, invasion, colony-forming potential and apoptosis. Our findings reveal a key molecular determinant of differences between PC and CRPC at the level of the transcriptome. Further, they establish PCAT5 as a novel oncogenic lncRNA in ERG-positive prostate cancers, with implications for defining CRPC biomarkers and new therapeutic interventions.

# Introduction

The most frequent genomic lesion in prostate cancers is deletion of 21q22 in 50% of cases resulting in overexpression of ERG, an ETS family transcription factor. A translocation following the deletion fuses the regulatory sequence of an androgen regulated gene, most often TMPRSS2, with the protein coding sequence of ERG bringing it under androgen regulation [1]. ERG is a critical proto-oncogene that disrupts the ability of the cells to differentiate when activated. ERG fusions also contribute to development of androgen-independence in prostate cancer through inducing repressive epigenetic programs via activation of a Polycomb methylatransferase EZH2, inhibiting AR expression, and disruption of androgen receptor signaling [2]. Overexpression of ERG, or other ETS transcription factors, such as ETV1, and ETV4 activates cell invasion programs [3]. ETS negative prostate cancers have rare alternate driving events, such as SKIL-activating rearrangements [4]. Generally, the molecular mechanisms of action for ERG are yet to be fully understood.

Recently, long non-coding RNA molecules that are mainly transcribed from the intergenic regions of the genome (lncRNAs) have become a focus in transcriptome studies of cancers [5]. These molecules form an integral part of many biological processes, often through interactions with the Polycomb complex which lead to silencing tumor suppressive functions [6], but many other mechanisms have also been described [7]. Few prostate cancer specific lncRNAs have been well characterized to date, particularly PCGEM1 [8], PRNCR1 [9], *PCAT1* [10] and *SChLAP1* [11]. PCAT1 is a regulator of cell proliferation and a target of the Polycomb Repressive Complex 2 (PRC2) that represses BRCA2 tumor suppressor and controls homologous recombination [12]. SChLAP1 antagonizes the regulatory functions of the SWI/SNF chromatin-modifying complex leading to increased invasiveness and metastasis in vitro and its expression predicts poor outcome in clinical setting [11].

We hypothesized that there is still a significant amount of previously unexplored transcriptomic differences between hormone-naive and castration resistant PC, especially in the expression patterns of long non-coding RNAs. To conduct the first comprehensive characterization of protein-coding genes, small RNAs and lncRNAs in these prostate cancers, we deep-sequenced transcriptomes of 12 benign prostatic hyperplasias (BPH), 28 untreated PCs, and 13 CRPCs. In addition to identifying several CRPC-specific lncRNAs, we discovered PCAT5, an ERG-regulated tumor growth associated lncRNA that is exclusively expressed in ERG-positive PCs and CRPCs. Its functional association in prostate cancer progression may partly explain how ERG exerts its widespread effect in gene regulation.

# Materials and Methods

### Patient samples and sequencing

Fresh-frozen tissue specimens from 12 benign prostatic hyperplasias (BPHs), 28 PCs, and 13 CRPCs were acquired from Tampere University Hospital (Tampere, Finland). The BPHs included both transition zone (n=4) and peripheral zone (n=8) samples received either by TURP or cystoprostatectomy, respectively, from patients without prostate cancer diagnosis. All cancer samples contained a minimum of 70% cancerous or hyperplastic epithelial cells. PC samples were obtained by radical prostatectomy and locally recurrent CRPCs by transurethral resection of the prostate sequenced. Libraries were prepared for paired-end analysis on the Illumina HiSeq 2000. On average, we obtained 110 million 90bp-long paired-end reads from the whole transcriptome sequencing (RNA-seq), and 8.2 million 50bp-long single-end reads from the small RNA sequencing (sRNA-seq). The sequencing reads were subsequently aligned to the human genome and expression estimates for all expressed transcripts were computed. On average were able to align 92% of the reads (and minimum of 84%) indicating sufficient quality reads from all samples (**Supplementary Table 1)**. More detailed description of the experimental setup can be found in Supplementary Methods.

### Transcriptome assembly

To fully characterize the wealth of expressed transcripts in different stages of prostate cancer, we assembled a consensus transcriptome from all the samples using Cufflinks [13] RABT (reference annotation based transcript) assembly approach with NCBI 37.2/hg19 genome build. Comparing the assembled prostate cancer transcriptome to all the exonic and intronic sequences in human reference transcriptomes (UCSC hg19, NCBI build 37.2, Ensembl GRCh37, Gencode version 12e) resulted in identification of 99,120 novel loci of expression. Transcripts overlapping exonic sequences were labeled as known sequences (and not included in the 99,120 novel loci), transcripts fully contained in an intron were labeled as intragenic (32,744 (33%)), and transcripts not overlapping with exonic or intronic sequences were labeled as intergenic (66,376 (67%)). To reduce the effect of noise, we filtered the lowly expressed transcripts (maximum normalized read count under 500), and included only transcripts that were differentially expressed across the tumor types using a negative binomial test and Mann-Whitney U-test (adjusted p<0.001 for both tests). Filtering reduced the number of loci to 152 intergenic and 25 intragenic prostate cancer associated novel loci of transcription that were expressed at a significant level and were differentially expressed between BPH and PC or PC and CRPC samples **(Supplementary Table 2)**. More detailed description of the data analysis can be found in Supplementary Methods.

While taking account the programmatically predicted sequences of the transcripts, we manually inferred putative exon-structures, different isoforms, and strandedness for 145 transcripts or isoforms merging some of the adjacent loci of transcription. The curation from 152 loci into 145 isoforms were made based on the recurrent splice junctions in the paired-end read data coinciding with canonical intron splice site motifs. We were able to infer these structural details only for about half of the loci. The rest of the loci may either encode functional single-exon transcripts or be parts of ambiguously expressed large genomic regions such as SChLAP1 [11]. Following the previously adopted nomenclature, we named the transcripts tentatively as TPCATs (Tampere Prostate Cancer Associated Transcripts) followed by chromosome and locus identifications **(Supplementary Table 2)**. The annotation process is described in Supplementary Methods.

# Results

### Comprehensive transcriptome analysis reveals alterations in key regulatory pathways

We integrated the sequencing data into a comprehensive view of the PC and CRPC transcriptomes. Hierarchical clustering (**Figure 1a**) and principal component analysis (PCA) (**Figure 1b**) of gene expression profiles separated BPH, PC and CRPC samples into distinct clusters. From PCA analysis, we observed two additional clusters that represented cancers with special features: one cluster contained two AR negative tumors, while another contained tumors with strong AR amplification. We looked for differentially expressed genes using Mann-Whitney U-test with threshold for significant difference $p<0.0001$, and absolute difference between medians of length-normalized read counts above 200 and log2-ratio above 1. In total, we identified 798 genes and 20 small RNAs differentially expressed between BPH and PC, and 330 genes and 43 small RNAs between PC and CRPC (**Supplementary Table 3**). Pathway analysis associated genes that were differentially expressed in PC compared to BPH to cytochrome p450 metabolism, cell adhesion and transforming growth factor (TGF) beta signaling. Altered processes between CRPC and PC were dominated by regulatory pathways in which NR4A1, EGR family, FOS, DUSP1 and ATF3 play a key role (**Supplementary Table 3**). These genes were overexpressed in PCs but not in CRPCs, and their mutual correlation (Pearson correlation > 0.9) indicated potentially shared regulation.

To highlight the pathway level changes in cell cycle and androgen regulation, we constructed pathway models of these processes and projected the observed expression changes onto these models. In cell cycle, we noted a strong combined overexpression of the proliferation markers MKI67, TOP2A, AURKA and EZH2 in half of CRPCs, suggesting a high proliferation rate in these tumors. This high proliferation rate was also reflected in the expression of cyclins CCNB1, CCNB2 and CCNE2, and the cyclin dependent kinase CDK1 (**Supplementary Figure 1**). In the androgen regulation pathway, we observed overexpression of androgen receptor (AR) in 7 of 13 CRPCs. The AR coactivator FOXA1 was overexpressed in untreated PC relative to BPH. Isozymes SRD5A1 and SRD5A2, responsible for testosterone-to-DHT conversion, showed respective up- and downregulation in CRPC. Enzymes AKR1C3 and AKR1C2, responsible for canonical androstenedione-to-testosterone reduction, were overexpressed in 30-50% of CRPCs, with associated overexpression of UGT2B15 and UGT2B17, enzymes responsible for glucuronidation of testosterone and DHT. Transcription factors ERG and ETV1 were overexpressed in 25 of 41 prostate cancers corresponding to previously established frequency of fusions with the androgen regulated TMPRSS2. [1] (**Supplementary Figure 2**)

### The expression patterns of novel long non-coding RNAs differentiate between PC and CRPC

Majority of the novel expressed loci were detected in CRPC only or in both PC and CRPC, but a few loci were expressed in all three sample groups, albeit at different rates, or were specific to the AR negative samples (**Figure 1c**). Over 30% of the transcripts were expressed on average at more than ten times higher level in CRPCs than in PCs or BPHs which we considered highly CRPC-specific expression pattern. Some of the transcripts were expressed in only few samples corresponding to outlier expression pattern. The specificities of the TPCAT expression patterns were further validated using available RNA-sequencing data from 21 PC cell lines [10], 24 normal tissues [14], 2 human embryonic stem cells (PolyA-selected and non-selected) [15], and two independent cohorts of PC tumors (n=30 and n=34, respectively) [10,16] **(Supplementary Table 2)**. Generally, TPCATs were minimally expressed in normal tissues, with testes most commonly being the normal tissue with the highest expression level. The expression patterns in cancer tissue were generally concordant in all three PC cohorts.

To investigate whether changes in DNA methylation or copy number bring about the expression of the novel transcripts in the samples that express them, we integrated DNA-sequencing and MeDIP-sequencing data from the same samples with the RNA-seq data (See **Supplementary Methods**). We computed Spearman correlations between transcript expression values and the copy number of the locus, and expression values and methylation values of nearby differentially methylated regions. In addition, we tested for differential expression between samples that had copy number aberrations at the locus versus samples that had normal copy number for each TPCAT using t-test. We required a significant correlation between the expression and copy number, and significantly differential expression between samples with normal copy number and samples with copy number aberration. Similar requirements were applied to methylation. None of the TPCATs were found to be significant taking account both criteria indicating that the expression differences of TPCATs were not explained by these factors. This suggesting that, at least in general, TPCATs are transcriptionally regulated and that their expression does not arise due to genetic alterations or changes in DNA methylation (**Supplementary Table 4**).

We wanted to find prostate cancer associated transcription factors that could act partly by regulating some of the lncRNAs we discovered. Spearman correlations were computed between the expression of the lncRNAs and eight transcription factors (ERG, AR, FOXA1, EZH2, HDAC1, HDAC2, HDAC3, RUNX2) for which public ChIP-sequencing data in PC cell lines were available for validating the regulatory association. The correlation analysis associated the expression of several TPCATs with the expression of these transcriptional regulators (**Supplementary Table 4**). The strongest positive correlation (r=0.69) was observed between *ERG* and transcript *TPCAT-10-36067* (officially termed *PCAT5*) **(Figure 1c).** Concordantly with ERG expression, PCAT5 was expressed in a subset of PCs and CRPCs (**Figure2a-b**). The expression was detected at a comparable frequency in both independent cohorts of PC, but not significantly in healthy tissues, including BPHs. The expression of *PCAT5* was quantified and validated in independent cohort of 76 primary PC samples as well as *ETV4*-positive PC-3 and *ERG*-positive VCaP cells using qRT-PCR (**Supplementary Figure 3**). Additionally, and the expression correlation between *PCAT5* and *ERG* was validated in this 76 sample set with ERG immunohistochemistry, and in LuCaP xenografts with qRT-PCR (r=0.78) (**Supplementary Figure 3**). Expressions of four additional CRPC-expressed multi-exon TPCATs were also validated with RT-PCR **(Supplementary Figures 4-5)**. Since ERG is a dominant feature in prostate cancers, we decided to concentrate our validation efforts to deciphering the exact structure of PCAT5, elucidating the regulatory connection between PCAT5 and ERG, and investigating the functional relevance of PCAT5.

### Inhibition of PCAT5 expression reduces growth, migration and invasion of ERG-positive PC cells

Based on spliced read alignments, we inferred a three-exon structure for *PCAT5* with no components of viral ORFs or other repetitive elements located on the exons **(Figure 3a)**. Both exon-exon junctions were validated with RT-PCR and Sanger sequencing in three clinical samples **(Supplementary Figure 3)**. To accurately identify both termini of the transcript, we performed 5’ and 3’ rapid amplification of cDNA ends (RACE). ORF analysis indicated that the transcript lacks protein coding potential. From available ChIP-sequencing data measured from ERG-positive VCaP cells **(Supplementary Table 4)**, we identified open chromatin histone markers, such as H3K4 trimethylation, and binding events of ERG and RNA polymerase II at proximal promoter of *PCAT5* **(Figure 3a)**. Conversely, no ERG binding or H3K4 trimethylation was found at the PCAT5 promoter in LNCaP cells which do not express PCAT5 **(Supplementary Figure 6)**. Sequence analysis revealed a canonical ETS family DNA-binding motif and a TATA-box coinciding with the locus that ERG was bound to, and a polyadenylation signal at the 3’-end of the transcript **(Figure 3a)**. We further validated the regulatory association by knocking down ERG in VCaP cells using an siRNA (**Figure 3b**) which led to 75% inhibition of PCAT5 expression (**Figure 3c**). Similarly, we validated the association between PCAT5 and another ETS-family transcription factor, ETV4, by knocking it down in ERG-negative PC-3 cells leading to comparable inhibition of PCAT5 expression (**Supplementary Figure 7**). These data indicate that PCAT5 is under direct regulation by ERG, and likely other ETS family transcription factors as well.

To characterize and validate the function of *PCAT5*, we suppressed its expression with two different siRNAs in two cell lines: PC-3 cells which expressed the transcript (**Figure 4a**), and 22Rv1 cells which did not express it. The genome-wide expression changes that the suppression induced to PC-3 cells were studied using expression arrays. Gene Ontology enrichment analysis indicated that cell cycle, mitosis and Aurora signaling were the most extensively affected processes **(Supplementary Table 5)**. Several functional assays validated the computationally identified biological processes: the knockdown dramatically decreased cell growth **(Figure 4b)** and invasiveness **(Figure 4c)**, and increased the rate of apoptosis **(Figure 4d).** In addition, colony formation **(Figure 4e)** and migration potential **(Figure 4f)** of the transfected PC-3 cells decreased substantially compared to non-transfected PC-3 cells. Conversely, the growth rate of 22Rv1 cells that do not express *PCAT5* was unaffected by the siRNA suppression as expected **(Supplementary Figure 8)** whereas the growth of ERG-positive DuCaP cells decreased after siRNA suppression of PCAT5 **(Supplementary Figure 9)**. These results suggest that *PCAT5* has a key role in regulating tumor growth and malignancy in ETS positive prostate cancers.

# Discussion

Hundreds of lncRNAs, for which little more than an expression pattern is known, have been discovered by RNA-sequencing and stored in databases such as NONCODE [17]. A growing interest towards lncRNAs in cancer research is sparked by the dozens of molecules that have been implicated as key players in cancer cells [5]. In prostate tumorigenesis, differential expression of hundreds of lncRNAs is already a recognized phenomenon [8, 9, 11]. However, the functional role of many cancer-associated lncRNAs remains undetermined. The expression of lncRNA may confer clinical information about disease outcomes and thus have utility as diagnostic tests. One prostate cancer specific biomarker lncRNA, PCA3, is currently in use [18]. Evidence for effectively targeting tumor-specific lncRNAs as a therapeutic regimen [19], such as the telomerase lncRNA *TERC*, are accumulating. Therefore, the characterization of the non-coding RNA species and their functions are clinically important.

To identify novel transcripts, a comparable experimental and computational approach was taken by Prensner and others which resulted in discovery of 121 lncRNAs in untreated prostate cancer [10]. Here, we extended the list of prostate tumor specific transcripts with 145 distinct molecular entities by including CRPC samples to the cohort and performing much deeper sequencing. Outlier-type expression patterns of many lncRNAs discovered in this paper may explain why many of them had not been discovered to this date despite the use of RNA-sequencing technologies. Further, many lncRNAs were expressed in moderate-to-low levels which may have caused previous studies to overlook them. Also, PCAT5 that was identified as a key molecule in ERG positive prostate cancers is quite lowly but consistently transcribed in other cohorts.

Integration with DNA-seq and MeDIP-seq data indicated that the expression of none of the novel transcripts correlated with copy number or DNA methylation status, and thus it seems that the expression of these transcripts is not driven by copy number changes or differential DNA methylation. For example, in cell lines that have open chromatin at *PCAT5* promoter likely express it due to a binding of an ETS family transcription factor. The mechanism is intriguing since *ERG* overexpression is one of the hallmark events of prostate cancer, whereas the mechanisms downstream of ERG remain poorly understood. Our siRNA experiments revealed that *PCAT5* affects both cell growth and invasiveness, which suggests that the transcript may be an integral mediator in the regulatory cascade downstream of ERG. While low expression level is probably not ideal for a biomarker, the strong phenotype combined with prostate cancer specificity, makes *PCAT5* a prospective target for therapy.

In conclusion, we performed the first transcriptomic analysis on CRPC and identified more than hundred novel lncRNAs that seem to be specific for either PC or CRPC. One of the lncRNAs, PCAT5, was shown to be regulated by ERG and have a dramatic effect on prostate cancer cells. Inclusion of more specimens, especially CRPCs, would likely result in identification of even more novel lncRNAs with outlier type of expression pattern. Biopsies of metastases might also reveal novel lncRNAs that are specific to these tumors and ones that are not expressed in primary tumors. However, the identified transcripts form an interesting pool of putative biomarker and mechanisms for prostate cancer progression.

# Acknowledgements

The authors express gratitude to Dr. Robert L. Vessella for the LuCaP xenograft data. The work was supported by grants from the Finnish Funding Agency for Technology and Innovation Finland Distinguished Professor programme (OYH, MN), Academy of Finland (project nos. 269474, and 132877 MN, project no. 251790 OYH, project no. 127187 TV), Sigrid Juselius Foundation (MN, TV), Emil Aaltonen Foundation (MA), Cancer Society of Finland (MN, TV). Competitive State Research Financing of the Expert Responsibility area of Tampere University Hospital (Grant 9P053 TLJT, Grant 9N087 TV), and EU-FP7 Marie Curie Integrated Training Network, PRO-NEST (TV), the National Institutes of Health (U24CA143835, WZ). We would like to thank CSC – IT Center for Science for providing computational resources.

## References

1. Tomlins SA, Rhodes DR, Perner S, Dhanasekaran SM, Mehra R, Sun XW, et al. Recurrent fusion of TMPRSS2 and ETS transcription factor genes in prostate cancer. Science. 2005;310:644-648.
2. Yu J, Yu J, Mani RS, Cao Q, Brenner CJ, Cao X, Wang X, Wu L, Li J, Hu M, Gong Y, Cheng H, Laxman B, Vellaichamy A, Shankar S, Li Y, Dhanasekaran SM, Morey R, Barrette T, Lonigro RJ, Tomlins SA, Varambally S, Qin ZS, Chinnaiyan AM. An integrated network of androgen receptor, polycomb, and TMPRSS2-ERG gene fusions in prostate cancer progression. Cancer Cell. 2010;17:443-454.
3. Tomlins SA, Laxman B, Dhanasekaran SM, Helgeson BE, Cao X, Morris DS, Menon A, Jing X, Cao Q, Han B, Yu J, Wang L, Montie JE, Rubin MA, Pienta KJ, Roulston D, Shah RB, Varambally S, Mehra R, Chinnaiyan AM. Distinct classes of chromosomal rearrangements create oncogenic ETS gene fusions in prostate cancer. Nature. 2007;448:595-599.
4. Annala M, Kivinummi K, Tuominen J, Karakurt S, Granberg K, Latonen L, Ylipää A, Sjöblom L, Ruusuvuori P, Saramäki O, Kaukoniemi KM, Yli-Harja O, Vessella RL, Tammela TLJ, Zhang W, Visakorpi T, Nykter M. Recurrent SKIL-activating rearrangements in ETS negative prostate cancer. Oncotarget. 2015. In press.
5. Prensner JR, Chinnaiyan AM. The emergence of lncRNAs in cancer biology. Cancer Discovery. 2011;1:391-407.
6. Rinn JL, Kertesz M, Wang JK, Squazzo SL, Xu X, Brugmann SA, Goodnough LH, Helms JA, Farnham PJ, Segal E, Chang HY. Functional demarcation of active and silent chromatin domains in human HOX loci by noncoding RNAs. Cell. 2007;129:1311-23.
7. Wang KC, Chang HY. Molecular mechanisms of long noncoding RNAs. Molecular Cell. 2011;43:904-14.

8. Srikantan V, Zou Z, Petrovics G, Xu L, Augustus M, Davis L, Livezey JR, Connell T, Sesterhenn IA, Yoshino K, Buzard GS, Mostofi FK, McLeod DG, Moul JW, Srivastava S. PCGEM1, a prostate-specific gene, is overexpressed in prostate cancer. PNAS. 2000;97:12216-21.

9. Chung S, Nakagawa H, Uemura M, Piao L, Ashikawa K, Hosono N, Takata R, Akamatsu S, Kawaguchi T, Morizono T, Tsunoda T, Daigo Y, Matsuda K, Kamatani N, Nakamura Y, Kubo M. Association of a novel long non-coding RNA in 8q24 with prostate cancer susceptibility. Cancer Science. 2011;102:245-252.

10. Prensner JR, Iyer MK, Balbin OA, Dhanasekaran SM, Cao Q, Brenner JC, et al. Transcriptome sequencing across a prostate cancer cohort identifies PCAT-1, an unannotated lincRNA implicated in disease progression. Nature Biotechnology. 2011;29:742-749.

11. Prensner JR, Iyer MK, Sahu A, Asangani IA, Cao Q, Patel L, et al. The long noncoding RNA SchLAP1 promotes aggressive prostate cancer and antagonizes the SWI/SNF complex. Nature Genetics. 2013;45:1392-1398.

12. Prensner JR, Chen W, Iyer MK, Cao Q, Ma T, Han S, Sahu A, Malik R, Wilder-Romans K, Navone N, Logothetis CJ, Araujo JC, Pisters LL, Tewari AK, Canman CE, Knudsen KE, Kitabayashi N, Rubin MA, Demichelis F, Lawrence TS, Chinnaiyan AM, Feng FY. PCAT-1, a long noncoding RNA, regulates BRCA2 and controls homologous recombination in cancer. Cancer Res. 2014;74:1651-60.

13. Trapnell C, Williams BA, Pertea G, Mortazavi A, Kwan G, van Baren MJ, et al. Transcript assembly and quantification by RNA-Seq reveals unannotated transcripts and isoform switching during cell differentiation. Nature Biotechnology. 2010;28:511-5.

14. Cabili MN, Trapnell C, Goff L, Koziol M, Tazon-Vega B, Regev A, Rinn JL. Integrative annotation of human large intergenic noncoding RNAs reveals global properties and specific subclasses. Genes & Development. 2011;24:1915-27.

15. ENCODE Project Consortium, Bernstein BE, Birney E, Dunham I, Green ED, Gunter C, Snyder M. An integrated encyclopedia of DNA elements in the human genome. Nature. 2012;489:57-74.

16. Kannan K, Wang L, Wang J, Ittmann MM, Li W, Yen L. Recurrent chimeric RNAs enriched in human prostate cancer identified by deep sequencing. PNAS. 2011;108:9172-9177.

17. Bu D, Yu K, Sun S, Xie C, Skogerbø G, Miao R, Xiao H, Liao Q, Luo H, Zhao G, Zhao H, Liu Z, Liu C, Chen R, Zhao Y. NONCODE v3.0: integrative annotation of long noncoding RNAs. Nucleic Acids Research. 2012;40:D210-5.

18. Hessels D, Schalken JA. The use of PCA3 in the diagnosis of prostate cancer. Nature Reviews Urology. 2009;6:255-261.

19. Li CH, Chen Y. Targeting long non-coding RNAs in cancers: progress and prospects. Int J Biochem Cell Biol. 2013;45:1895-1910.

# Figure legends

**Figure 1.** Expression level characterization of prostate cancers. (**a**) Hierarchical clustering of annotated genes reveals distinct gene expression signatures for BPH (green), PC (yellow), and locally recurrent CRPC (red). High expressions of key marker genes, such as ERG and AR, have been highlighted for all the tumors in red, and low expression in blue, different levels of shade indicating the level of expression difference from the median. Two tumors (PC_6864 and CRPC_531, purple) were negative for AR expression and positive for neuronal differentiation marker HES6. (**b**) Principal component analysis. BPH, PC and CRPC samples are well separated into distinct clusters based on their gene expression profiles. AR negative tumors (PC_6864, CRPC_531) as well as tumors with strong AR amplification and overexpression (CRPC_530, CRPC_278) formed separate clusters. (**c**) Association of found transcripts to disease phenotypes. A number of transcripts were associated with *ERG* positive PCs and CRPCs, including *PCAT5*. In addition, many transcripts were CRPC-specific and few showed specificity to untreated PCs. Most transcripts were found in all cancer tissue types.

**Figure 2.** Expression patterns of PCAT5. (**a**) Association of PCAT5 expression to prostate cancer was confirmed by analyzing additional prostate cancer and healthy tissue RNA-seq data sets. (**b**) ERG and PCAT5 expressions derived from our RNA-seq data were plotted for each sample. A cutoff of 1000 RPKs was chosen to differentiate ERG negative and ERG positive samples. The ERG negative pool contained all the BPH samples, 12 PCs, and 6 CRPC whereas the ERG positive pool contained 15 PCs and 6 CRPC samples.

**Figure 3.** Sequence analysis of PCAT5, located in 10p11.21. (**a**) Regulatory properties of *PCAT5* were investigated using ChIP-sequencing data of H3K4me3, ERG, and POL2 from *PCAT5*-positive VCaP cells (blue), and detailed expression profiles in *ERG*-negative and *ERG*-positive samples, and in an independent PC cohort (gray). The data were overlaid onto the inferred exon structure of *PCAT5* (in red)

indicating open chromatin coinciding with ERG and POL2 binding events in the promoter of VCaP cells, and active expression in *ERG* positive samples compared to *ERG* negative samples. An ETS DNA-binding domain and TATA box were identified at the suspected promoter region and a Poly-A signal sequence at the end of third exon. (**b**) ERG and (**c**) PCAT5 expression after 50nM ERG-siRNA or scrambled CTRL-siRNA treatment in VCaP cells. Error bars, s.e.m.; **p<0.0083; ***p<0.001, unpaired two-tailed t-test (n=3).

**Figure 4.** Functional validation of PCAT5. (**a**) Successful silencing of PCAT5 using multiple siRNA knockdowns were validated using qRT-PCR. (**b**) Growth of *PCAT5* positive PC-3 cell line was completely inhibited by siRNAs targeting the transcript. (**c**) Invasiveness of PC-3 cells was reduced by the siRNA knockdown. (**d**) Annexin V assay indicated an increased rate of apoptosis after the knockdown. Error bars, s.e.m.; *P<0.05; **P<0.01; ***P<0.001, unpaired two-tailed t-test. (**e**) Colony formation was significantly reduced in the PCAT5-deficient PC-3 cells. (**f**) Wound healing assay (triplicates, representative experiment shown) indicated a significantly impaired migration ability.

Figure 1

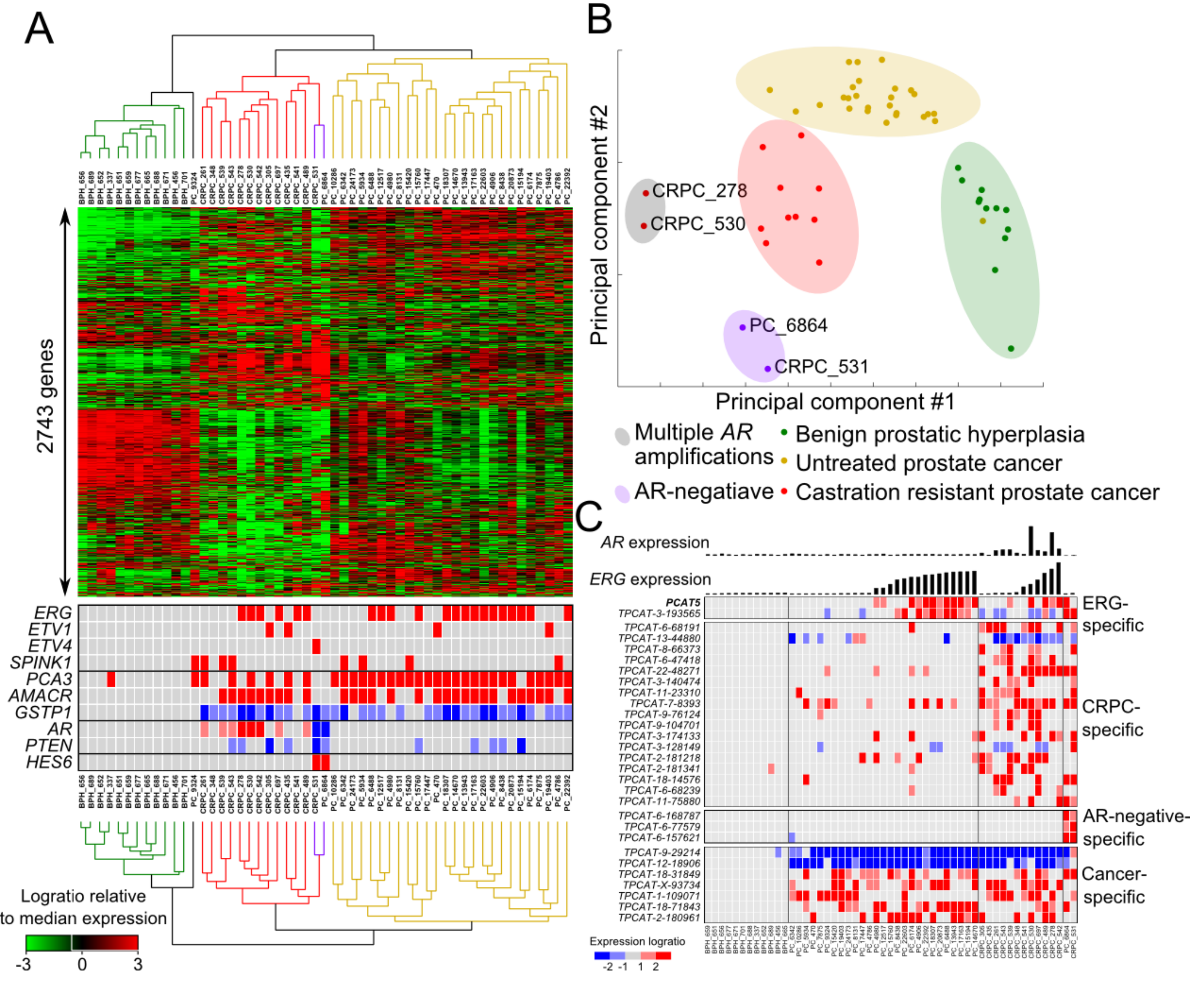
A
2743 genes
ERG
ETV1
ETV4
SPINK1
PCA3
AMACR
GSTP1
AR
PTEN
HES6
Logratio relative
to median expression
-3
0
3
BPH_656
BPH_689
BPH_652
BPH_337
BPH_651
BPH_659
BPH_677
BPH_665
BPH_688
BPH_671
BPH_456
BPH_701
PC_9324
CRPC_261
CRPC_348
CRPC_539
CRPC_543
CRPC_278
CRPC_530
CRPC_542
CRPC_305
CRPC_697
CRPC_435
CRPC_541
CRPC_489
CRPC_531
PC_6864
PC_10286
PC_6342
PC_24173
PC_5934
PC_6488
PC_12517
PC_4980
PC_8131
PC_15420
PC_15760
PC_17447
PC_470
PC_18307
PC_14670
PC_13943
PC_17163
PC_22603
PC_4906
PC_8438
PC_20873
PC_15194
PC_6174
PC_7875
PC_19403
PC_4786
PC_22392
B
Principal component #2
Principal component #1
CRPC_278
CRPC_530
PC_6864
CRPC_531
Multiple AR amplifications
AR-negatiave
● Benign prostatic hyperplasia
● Untreated prostate cancer
● Castration resistant prostate cancer
C
AR expression
ERG expression
PCAT5
TPCAT-3-193565
ERG-specific
TPCAT-6-68191
TPCAT-13-44880
TPCAT-8-66373
TPCAT-6-47418
TPCAT-22-48271
TPCAT-3-140474
TPCAT-11-23310
TPCAT-7-8393
TPCAT-9-76124
TPCAT-9-104701
TPCAT-3-174133
TPCAT-3-128149
TPCAT-2-181218
TPCAT-2-181341
TPCAT-18-14576
TPCAT-6-68239
TPCAT-11-75880
CRPC-specific
TPCAT-6-168787
TPCAT-6-77579
TPCAT-6-157621
AR-negative-specific
TPCAT-9-29214
TPCAT-12-18906
TPCAT-18-31849
TPCAT-X-93734
TPCAT-1-109071
TPCAT-18-71843
TPCAT-2-180961
Cancer-specific
Expression logratio
-2 -1 1 2

Figure 2

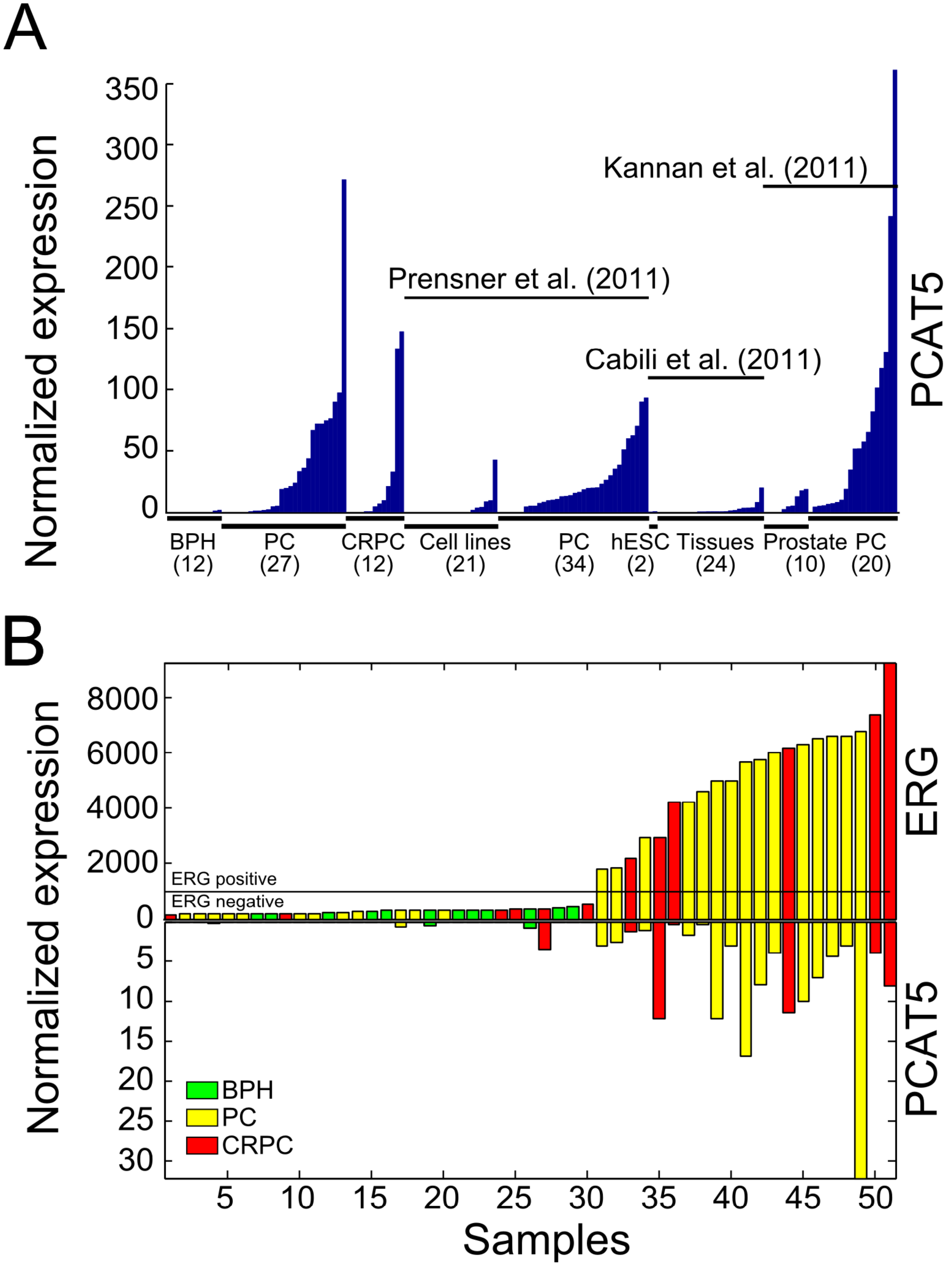
A
Normalized expression
350
300
250
200
150
100
50
0
PCAT5
Kannan et al. (2011)
Prensner et al. (2011)
Cabili et al. (2011)
BPH (12)
PC (27)
CRPC (12)
Cell lines (21)
PC (34)
hESC (2)
Tissues (24)
Prostate (10)
PC (20)
B
Normalized expression
8000
6000
4000
2000
0
5
10
15
20
25
30
ERG positive
ERG negative
ERG
PCAT5
🟩 BPH
🟨 PC
🟥 CRPC
5
10
15
20
25
30
35
40
45
50
Samples

Figure 3

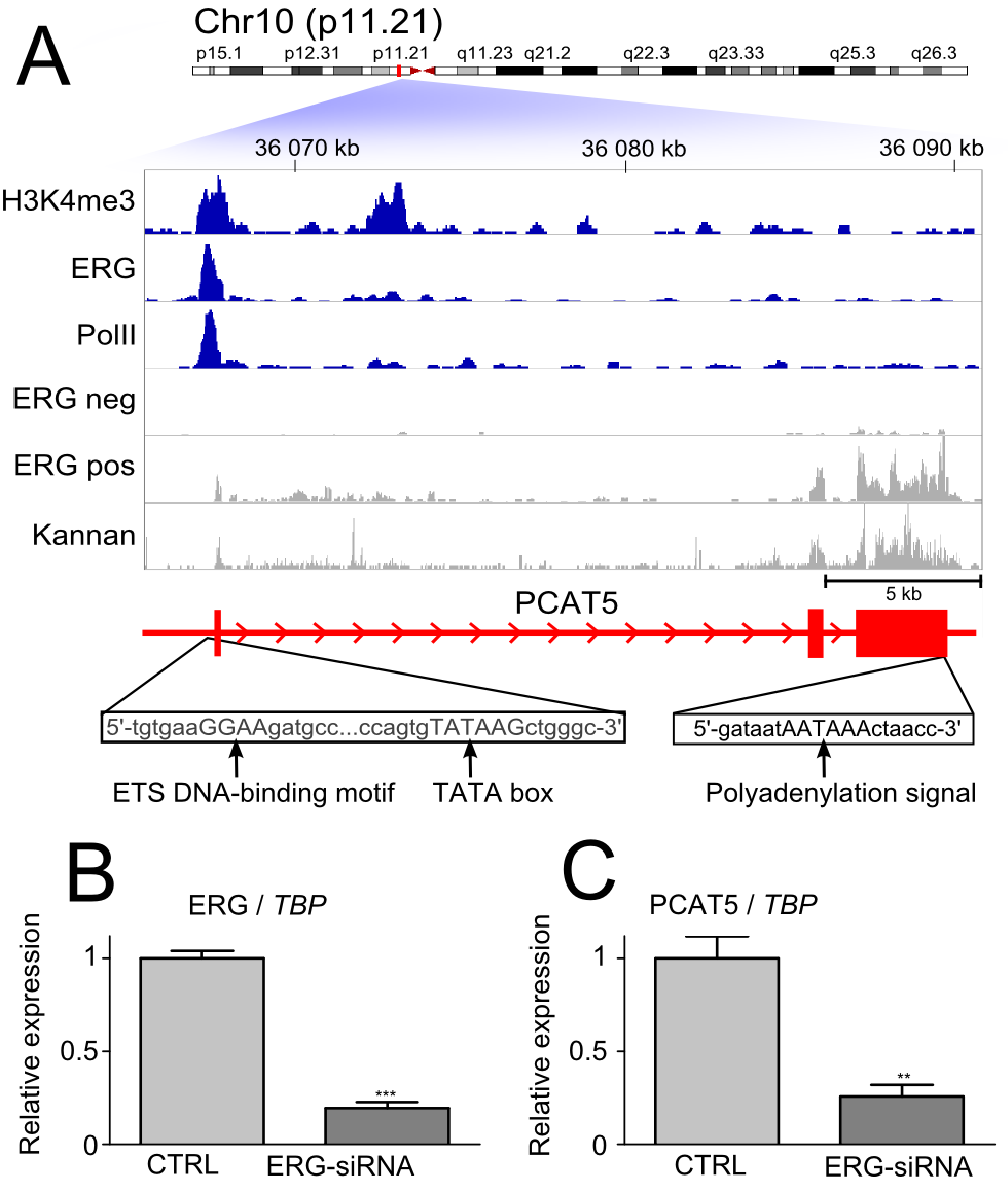
A
Chr10 (p11.21)
p15.1
p12.31
p11.21
q11.23
q21.2
q22.3
q23.33
q25.3
q26.3
36 070 kb
36 080 kb
36 090 kb
H3K4me3
ERG
PolII
ERG neg
ERG pos
Kannan
5 kb
PCAT5
5'-tgtgaaGGAAgatgcc...ccagtgTATAAGctgggc-3'
5'-gataatAATAAActaacc-3'
ETS DNA-binding motif
TATA box
Polyadenylation signal
B
ERG / *TBP*
Relative expression
1
0.5
0
***
CTRL
ERG-siRNA
C
PCAT5 / *TBP*
Relative expression
1
0.5
0
**
CTRL
ERG-siRNA

Figure 4

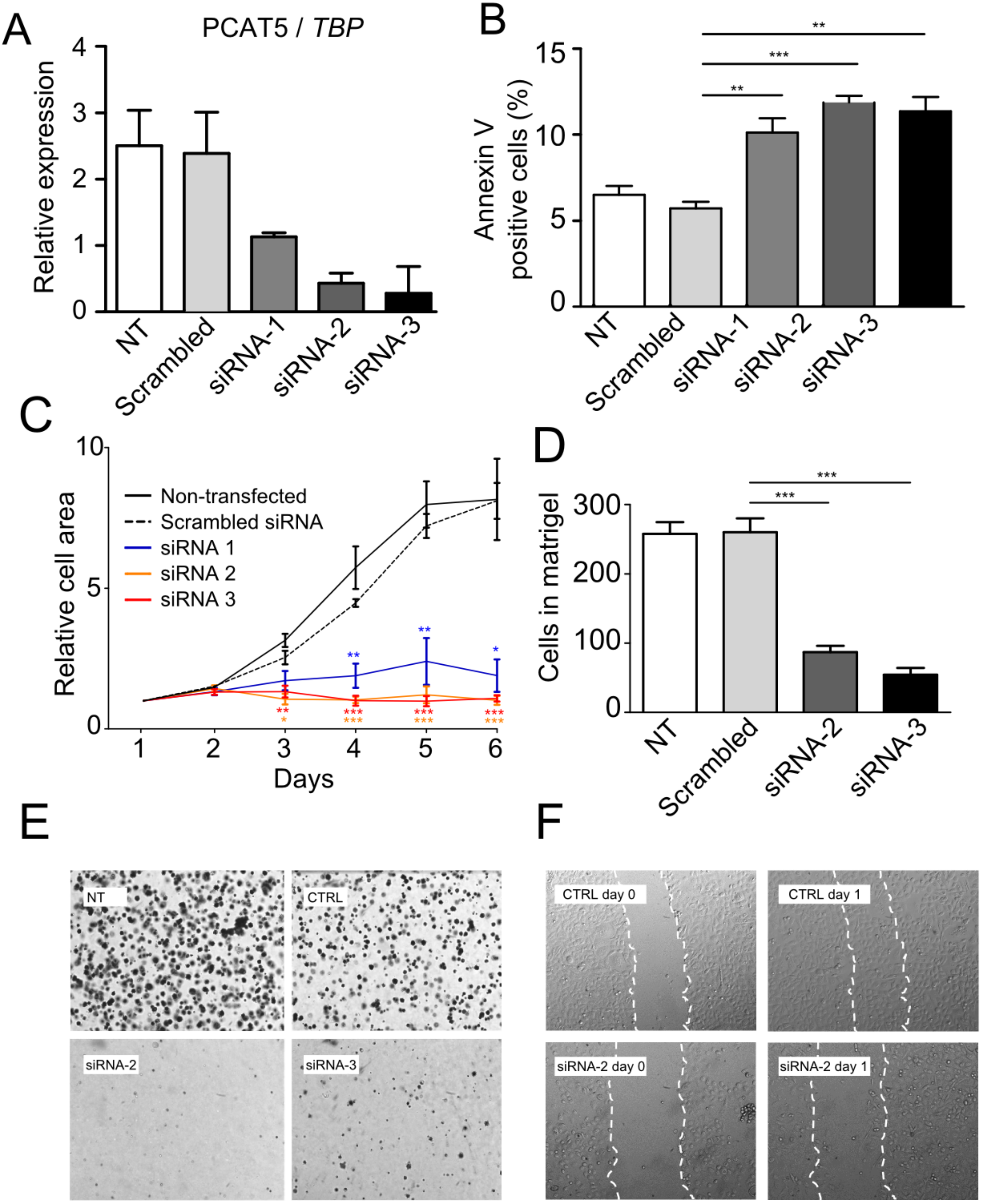
A
PCAT5 / TBP
Relative expression
0
1
2
3
4
NT
Scrambled
siRNA-1
siRNA-2
siRNA-3
B
Annexin V positive cells (%)
0
5
10
15
**
***
**
NT
Scrambled
siRNA-1
siRNA-2
siRNA-3
C
Relative cell area
0
5
10
Non-transfected
Scrambled siRNA
siRNA 1
siRNA 2
siRNA 3
**
**
*
**
*
***
***
***
***
***
***
1
2
3
4
5
6
Days
D
Cells in matrigel
0
100
200
300
***
***
NT
Scrambled
siRNA-2
siRNA-3
E
NT
CTRL
siRNA-2
siRNA-3
F
CTRL day 0
CTRL day 1
siRNA-2 day 0
siRNA-2 day 1